



HAL
open science

Limb scatter ozone retrieval from 10 to 60 km using a Multiplicative Algebraic Reconstruction Technique

D. A. Degenstein, A. E. Bourassa, C. Z. Roth, E. J. Llewellyn

► **To cite this version:**

D. A. Degenstein, A. E. Bourassa, C. Z. Roth, E. J. Llewellyn. Limb scatter ozone retrieval from 10 to 60 km using a Multiplicative Algebraic Reconstruction Technique. *Atmospheric Chemistry and Physics Discussions*, 2008, 8 (3), pp.11853-11877. hal-00304265

HAL Id: hal-00304265

<https://hal.science/hal-00304265v1>

Submitted on 18 Jun 2008

HAL is a multi-disciplinary open access archive for the deposit and dissemination of scientific research documents, whether they are published or not. The documents may come from teaching and research institutions in France or abroad, or from public or private research centers.

L'archive ouverte pluridisciplinaire **HAL**, est destinée au dépôt et à la diffusion de documents scientifiques de niveau recherche, publiés ou non, émanant des établissements d'enseignement et de recherche français ou étrangers, des laboratoires publics ou privés.

**MART Limb Scatter
Ozone Retrieval**

D. A. Degenstein et al.

Limb scatter ozone retrieval from 10 to 60 km using a Multiplicative Algebraic Reconstruction Technique

D. A. Degenstein¹, A. E. Bourassa², C. Z. Roth¹, and E. J. Llewellyn¹

¹Institute of Space and Atmospheric Studies, Saskatchewan, Canada

²Science Systems and Applications, Inc., Hampton, VA, USA

Received: 12 March 2008 – Accepted: 4 May 2008 – Published: 13 June 2008

Correspondence to: D. A. Degenstein (doug.degenstein@usask.ca)

Published by Copernicus Publications on behalf of the European Geosciences Union.

Title Page

Abstract

Introduction

Conclusions

References

Tables

Figures

◀

▶

◀

▶

Back

Close

Full Screen / Esc

Printer-friendly Version

Interactive Discussion



Abstract

The OSIRIS instrument onboard the Odin spacecraft routinely measures vertical profiles of spectrally dispersed, limb scattered sunlight from the upper troposphere into the lower mesosphere. These measurements are used to retrieve the ozone number density vertical profile over the altitude range from 10 to 60 km using the SaskMART Multiplicative Algebraic Reconstruction Technique, which is a one dimensional modification of an existing two-dimensional tomographic retrieval algorithm. This technique allows for the consistent merging of the absorption information from radiance measurements at wavelengths in the Chappuis and the Hartley-Huggins bands at each iteration of the inversion. The effectiveness of the retrieval is demonstrated using a set of coincident SAGE II occultation measurements that show a mean bias of less than 2% from 18 to 53 km.

1 Introduction

In recent years multiple satellite instruments have been developed that measure the spectrum of limb scattered sunlight at ultraviolet, visible and near-infrared wavelengths. The limb scatter data set allows for the retrieval of trace gas and aerosol profiles at a vertical resolution comparable to that of occultation measurements, but with significantly better global coverage. The first retrievals of ozone from satellite limb radiance measurements were made in the upper atmosphere by the Ultraviolet Spectrometer (UVS) on the Solar Mesospheric Explorer (SME) (Rusch et al., 1984). The demonstration flight instruments Shuttle Ozone Limb Sounding Experiment/Limb Ozone Retrieval Experiment (SOLSE/LORE) measured the limb radiance at several wavelengths in the Hartley-Huggins and Chappuis bands (McPeters et al., 2000). The vertical profile of the ozone density was retrieved from these measurements using normalized pair and triplet combinations of the radiances. The first routinely retrieved limb-scatter ozone product was made with data from the Optical Spectrograph and InfraRed Imaging Sys-

ACPD

8, 11853–11877, 2008

MART Limb Scatter Ozone Retrieval

D. A. Degenstein et al.

Title Page

Abstract

Introduction

Conclusions

References

Tables

Figures

◀

▶

◀

▶

Back

Close

Full Screen / Esc

Printer-friendly Version

Interactive Discussion



tem (OSIRIS) using a triplet combination of Chappuis band wavelengths to retrieve ozone densities from the troposphere up to 35 km (von Savigny et al., 2003). The Scanning Imaging Absorption Spectrometer for Atmospheric Cartography (SCIAMACHY) on Envisat (Bovensmann et al., 1999) is currently operational and routinely retrieves stratospheric/mesospheric ozone from limb radiance spectra in a similar fashion. The Stratospheric Aerosol and Gas Experiment (SAGE) III primarily retrieves trace gas profiles by solar occultation, but has the ability to measure the limb scatter radiances for retrieval of ozone and other species (Rault, 2005). The limb scatter technique is to be used in an operational sense with the upcoming launch of Ozone Mapping and Profiler Suite (OMPS) on the NPOESS Preparatory Project (Flynn et al., 2004).

In this work we present a new technique for the retrieval of ozone vertical profiles from 10 to 60 km using limb scatter radiances measured by the OSIRIS instrument. A key feature of this algorithm is that it allows for the simultaneous merging of the information contained within the visible and ultraviolet ozone absorption bands in a consistent manner. This is done using a set of weighting factors that specify the importance of each line of sight and each spectral measurement to the retrieval at each altitude of the profile. As part of this work, we introduce a methodology, based on the physics of the measurement, for the choosing of these weighting factors.

We demonstrate the success of this technique as applied to the OSIRIS measurements through comparison of these retrievals with near coincident SAGE II occultation measurements.

2 The Measurements

The Canadian built OSIRIS instrument is onboard the Odin satellite and has been fully operational since shortly after launch on 21 February 2001. The spectrograph module measures the limb scattered sunlight dispersed over a wavelength range from 280 to 800 nm at 1 nm resolution. In normal operational mode, OSIRIS scans the limb from 7 to 70 km tangent altitude at approximately 0.75 km/s. The Odin orbit is

Title Page

Abstract

Introduction

Conclusions

References

Tables

Figures

◀

▶

◀

▶

Back

Close

Full Screen / Esc

Printer-friendly Version

Interactive Discussion



circular and sun-synchronous at an altitude near 600 km with a period of 96 min. The orbital inclination of 98 degrees from the equator provides near-global coverage as the corresponding sampled latitude range for nominal on-track instrument pointing is from 82 degrees S to 82 degrees N. The local time of the ascending node, i.e. the northward equatorial crossing, is 18:00 h. For more information on the Odin satellite and the OSIRIS instrument see [Murtagh et al. \(2002\)](#) and [Llewellyn et al. \(2004\)](#) respectively.

This work presents a method for the retrieval of vertical ozone number density profiles from OSIRIS limb radiance profiles. Examples of the OSIRIS measurements from a typical limb scan are shown in Fig. 1 where the radiance is plotted as a function of tangent altitude. The left panel of the figure shows radiance profiles at selected wavelengths within the Hartley-Huggins absorption band. The right panel shows three profiles from the Chappuis band absorption feature. The tangent altitude below which the limb radiance profile becomes roughly constant is known as the knee. This is the minimum altitude probed at that wavelength as it is the point where the optical depth becomes large. It is clear from Fig. 1 that the UV measurements sample lower altitudes at longer wavelengths due to the decreasing ozone cross section, and that at the Chappuis wavelengths, it is still optically thin down to below 10 km.

The radiance profiles shown in Fig. 1 are combined to form the measurement vector. In a fashion similar to the technique employed by [Flittner et al. \(2000\)](#), measurement vector elements are formed using radiance profiles that are normalized at a reference tangent altitude. In the Hartley-Huggins region, radiances are used in pairs defined as the difference between the logarithm of a normalized measurement at an absorbing wavelength, $\tilde{I}(j, \lambda_{\text{abs}})$, and a similarly normalized measurement at a reference wavelength where the ozone absorption is very weak, $\tilde{I}(j, \lambda_{\text{ref}})$. Thus, the measurement vector element is,

$$y_{jk} = \ln \left(\frac{\tilde{I}(j, \lambda_{\text{ref}})}{\tilde{I}(j, \lambda_{\text{abs}})} \right). \quad (1)$$

In this notation, \tilde{I} represents a normalized radiance profile and j denotes a measured

**MART Limb Scatter
Ozone Retrieval**

D. A. Degenstein et al.

Title Page

Abstract

Introduction

Conclusions

References

Tables

Figures

◀

▶

◀

▶

Back

Close

Full Screen / Esc

Printer-friendly Version

Interactive Discussion



tangent altitude, i.e. a line of sight. The measurement vector elements are indexed by two subscripts, j and k . Again, j represents a tangent altitude, and k is a number that represents a pair/triplet combination. For example, in this work we use seven pairs and two triplets such that k ranges from 0 to 8.

5 At Chappuis band wavelengths, triplets are formed as the difference between the mean of the natural logarithm of two weakly absorbed normalized radiance profiles and the natural logarithm of the normalized radiance profile measured at a wavelength near the peak of the Chappuis cross section,

$$y_{jk} = \ln \left(\frac{\sqrt{\tilde{I}(j, \lambda_{\text{ref}_1}) \tilde{I}(j, \lambda_{\text{ref}_2})}}{\tilde{I}(j, \lambda_{\text{abs}})} \right). \quad (2)$$

10 The two reference wavelengths are taken on either side of the peak absorption. A summary of the measurement vector elements used in this work is provided in Table 1.

3 The SaskMART technique

The SaskMART technique is a type of Multiplicative Algebraic Reconstruction Technique (MART) that iteratively updates the atmospheric state parameter using the ratio of observed and modelled measurement vector elements. In a fashion similar to a non-linear relaxation technique (Chahine, 1972), the sensitivity of the measurement vector to the state parameter must be positive; thus the pair and triplet definitions given above are the inverse of those used in previous work (e.g. Flittner et al., 2000; von Savigny et al., 2003).

20 An important feature of the SaskMART algorithm is that more than one measurement vector element can be used to retrieve the state parameter at any altitude. At each iteration, the multiplicative factor used to update the current atmospheric state at each altitude is a weighted average of all the ratios of observed and modelled measurement vector elements that are significant to the retrieved value.

Title Page

Abstract

Introduction

Conclusions

References

Tables

Figures

◀

▶

◀

▶

Back

Close

Full Screen / Esc

Printer-friendly Version

Interactive Discussion



3.1 Development

The SaskMART equation,

$$x_i^{(n+1)} = x_i^{(n)} \sum_k \left(\sum_j \left(\frac{y_{kj}^{\text{obs}}}{y_{kj}^{\text{mod}}} W_{kji} \right) \right), \quad (3)$$

has been presented in various forms in previous works (Degenstein et al., 2003; Degenstein et al., 2004; Bourassa et al., 2007; Roth et al., 2007) associated with the retrieval of geophysical quantities from OSIRIS radiance measurements. In this application, $x_i^{(n)}$ is the ozone number density at an altitude denoted by i after the n^{th} iteration. The observed and modelled measurement vectors are denoted by y_{jk} , where j corresponds to a tangent altitude element of the k^{th} pair/triplet combination. The W_{kji} terms in Eq. (3) are weighting factors that determine the importance of the k^{th} pair/triplet combination and the j^{th} line of sight to the ozone density at the altitude i . At each altitude the sum over k and j of the weighting factors, W_{kji} , is unity.

The line of sight and pair/triplet weighting factors terms can be considered independently such that Eq. (3) can also be written as,

$$x_i^{(n+1)} = x_i^{(n)} \sum_k \left(W_{ki} \sum_j \left(\frac{y_{kj}^{\text{obs}}}{y_{kj}^{\text{mod}}} W_{ji} \right) \right), \quad (4)$$

where the W_{ki} term indicates the importance of the particular pair/triplet combination, k , to the retrieval at altitude i . The W_{ji} term allows more than one line of sight to contribute directly to the retrieved value at that altitude. Similarly, the summation of W_{ki} over k and W_{ji} over j are both unity. This follows Roth et al. (2007), where the SaskMART equation is discussed in two distinct parts. The first part, corresponding to

Title Page

Abstract

Introduction

Conclusions

References

Tables

Figures

◀

▶

◀

▶

Back

Close

Full Screen / Esc

Printer-friendly Version

Interactive Discussion



the inner sum in Eq. (4),

$$\alpha_{ik} = \sum_j \left(\frac{y_{kj}^{\text{obs}}}{y_{kj}^{\text{mod}}} W_{ji} \right), \quad (5)$$

is defined for a single pair/triplet profile, i.e. a given k , and determines the ratio

$$\alpha_{ik} = \frac{x_{ik}^{(n+1)}}{x_{ik}^{(n)}}. \quad (6)$$

- 5 This ratio, α_{ik} , is a multiplicative adjustment for iteratively updating x_i based on information from the k^{th} pair/triplet only. The notation x_{ik} is used to indicate this partial solution, which is for a given k , from the full solution that uses all pair/triplet combinations.

10 The second part of the SaskMART equation, the outer sum of Eq. (4), can then be written in terms of α_{ik} as,

$$\alpha_i = \sum_k (W_{ki} \alpha_{ik}), \quad (7)$$

where each multiplicative factor α_{ik} is weighted by the importance of the k^{th} pair/triplet for the retrieval at altitude i . Thus, α_i is the final multiplicative value,

$$\alpha_i = \frac{x_i^{(n+1)}}{x_i^{(n)}}, \quad (8)$$

- 15 that is used to update the state parameter at each iteration.

3.2 Combining multiple lines of sight

In previous work by Roth et al. (2007), where only Chappuis band information was used, the authors found it sufficient to allow three lines of sight, corresponding to successively lower tangent altitudes, to influence the retrieval at any given altitude. We

Title Page

Abstract

Introduction

Conclusions

References

Tables

Figures

◀

▶

◀

▶

Back

Close

Full Screen / Esc

Printer-friendly Version

Interactive Discussion



also follow this approach in this work such that elements W_{ij} in Eq. (4) are non-zero only if j represents the line of sight tangent through altitude i or the next two successively lower tangent altitudes. Likewise, we have followed the convention of Roth et al. (2007) and assigned $W_{i,j}$ a weight of 0.6, $W_{i,i-1}$ a weight of 0.3 and $W_{i,i-2}$ a weight of 0.1 as these roughly correspond to normalized values from the path length matrix.

3.3 Combining multiple pairs and triplets

As discussed in Sect. 2, in the limb geometry different wavelengths probe different altitude ranges based on the optical depth along the line of sight. At absorbing wavelengths, this is primarily a function of the strength of the ozone cross section. In combining multiple pairs and triplets for the retrieval, it is important that each measurement contributes only over the altitude range where lines of sight have a relatively large sensitivity to ozone. Based on this, we have developed a straight forward methodology for determining the altitude range over which each pair/triplet has non-zero weighting in the inversion.

The minimum altitude for each Hartley-Huggins band pair is determined by the location of the knee in the radiance profile of the absorbing wavelength (it is assumed that the knee in the reference wavelengths is below this altitude). The knee altitude is a somewhat weak function of the ozone profile; however, it is sufficient to choose an altitude corresponding to an average profile. Because there is no knee in the radiance profiles in the Chappuis band from 10 to 60 km, the minimum altitude of the two triplets we use in this work is set to 10 km, i.e. the lower retrieval boundary. The minimum altitude of the pairs formed from Hartley-Huggins band radiances decreases with wavelength from 47 km at 292 nm to 18 km at 331 nm. All values are summarized in Table 1. The normalization tangent altitude of the Chappuis band triplets is set to 33 km. At this altitude the ozone absorption is becoming significantly weak. As well, there is some potential for contamination from low signal to noise and stray light at these wavelengths above this altitude. The Hartley-Huggins band pairs are normalized at successively higher tangent altitudes such that the maximum value of the pair,

Title Page

Abstract

Introduction

Conclusions

References

Tables

Figures

◀

▶

◀

▶

Back

Close

Full Screen / Esc

Printer-friendly Version

Interactive Discussion



which occurs at the minimum altitude, is approximately 1.0. In an approximate sense, this represents a distance of one optical depth from the normalization altitude to the minimum altitude. The important effect of this scaling is that systematic errors in the forward model are minimized by using a normalization tangent altitude near the retrieval points. Again, see Table 1 for a full list of the normalization altitudes.

Finally, the maximum altitude for which each pair/triplet has a non-zero weight is chosen as 5 km below the normalization tangent altitude. It is important that the pair/triplet is not used in close proximity to the normalization because, by definition, the pairs and triplets, and hence the sensitivity, approach zero at the normalization point. As well, because the MART iterations are based on the ratio of the observed and modelled measurement vectors, it is wise to avoid the division of two small numbers in consideration of the noise that will be present in the observation. Fig. 2 shows the pair and triplet values constructed from the OSIRIS radiances shown in Fig. 1. The pairs using absorbing wavelengths at 292, 302, 306, 309, 315, and 322 nm profiles increase from zero at the normalization tangent altitude to a value near 1.0 at the minimum altitude. Two Chappuis band triplets are used in the retrieval but they are almost indistinguishable on this plot so only one is shown.

The pair constructed using the 331 nm radiance profile was chosen in a similar fashion; however as the ozone cross section is significantly weaker at this wavelength, the location of the knee is not as obvious. We have chosen 18 km as the minimum altitude for this pair. This creates significant overlap between the region that the Chappuis and Huggins band information is being used and is of great benefit for the consistency of the inversion in the transition region between the visible and ultraviolet wavelengths. The sensitivity of the 331 nm radiance to ozone at these low altitude is still significant. In fact, as shown in Fig. 3, the value of the Huggins band cross section at 331 nm is very similar to the peak of the absorption in the Chappuis band. The similar nature of the ozone sensitivity at these two wavelengths is reflected in the comparable shapes of the profile of the 331 nm pair and the Chappuis triplet shown in Fig. 2. Because the cross section at this wavelength is significantly less than for the other Hartley-Huggins

**MART Limb Scatter
Ozone Retrieval**

D. A. Degenstein et al.

[Title Page](#)[Abstract](#)[Introduction](#)[Conclusions](#)[References](#)[Tables](#)[Figures](#)[◀](#)[▶](#)[◀](#)[▶](#)[Back](#)[Close](#)[Full Screen / Esc](#)[Printer-friendly Version](#)[Interactive Discussion](#)

wavelengths that are used, the normalization altitude was chosen at 42 km to limit the contribution to an altitude range of approximately 20 km.

3.4 Setting the weighting factors

As explained in the previous section, the information from each pair and triplet shown in Fig. 2 is used for the retrieval over different, overlapping altitude ranges. The weighting factors, W_{ik} , in the SaskMART algorithm specify the relative contribution of each pair/triplet, k , as a function of altitude, where at each altitude, i , the sum of the weighting factors over k must equal unity. As part of this work we have found that it is important that the contribution from each pair/triplet is increased and decreased slowly over an altitude range so that small systematic errors in the forward model that vary with wavelength and altitude do not cause oscillatory structure in the retrieved profile. Thus the weighting factor for each pair/triplet is increased slowly from zero at the minimum altitude to the altitude where it has maximum significance for the retrieval and then slowly decreased to zero at the maximum altitude. For the highest altitude pair and the lowest altitude triplets the weighting factor is largest at the upper and lower retrieval boundary respectively. Fig. 4 is a plot of the weighting factors assigned to each of the pair and triplets used in this work. To create these weighting factors, we have used a roughly linear trend over 5–8 km to increase and decrease the weighting factor in each case from the minimum and maximum altitudes, while maintaining a unity sum of the weighting factors at each altitude. A second consideration in the creation of these weighting factors was to use information from at least three pairs or triplets at each altitude. Again the upper and lower boundaries are a special case. It is important to note that these factors do not have any direct mathematical relationship to either the averaging kernel or the Jacobian matrix.

We should also note that we have found, through significant testing, that it is possible to use similar, yet different weighting factors with very minimal impact on the retrieved solution. Especially in the case of an instrument with lower signal to noise, the addition of more pairs and triplets is certainly a good idea and a new set of weighting factors

Title Page

Abstract

Introduction

Conclusions

References

Tables

Figures

◀

▶

◀

▶

Back

Close

Full Screen / Esc

Printer-friendly Version

Interactive Discussion



can be determined using the same methodology. The weighting factors presented in this work are a sample set that is sufficient for use with the OSIRIS measurements.

4 Implementation details

4.1 The radiative transfer model

5 The radiative transfer model used in this work for the forward simulation of the limb radiances used to construct the measurement vector pair and triplet elements is the SASKTRAN model (Bourassa et al., 2008). SASKTRAN is a spherical shell, arbitrary order multiple scatter model that simulates the effects of absorbing gases and strato-
10 spheric sulphate aerosols on the propagation of uv-visible radiation through the atmosphere. The SASKTRAN model has been demonstrated by Bourassa et al. (2008) to agree well with the other similar models compared by Loughman et al. (2004). The ozone cross section used in SASKTRAN for this work is from Burrows et al. (1999). For the results presented in this paper the order of the multiple scatter calculation is limited to three scattering events, which is more than sufficient for the altitudes and
15 wavelengths that are considered.

4.2 The retrieval grid

The OSIRIS instrument scans the limb at a relatively constant rate; however, the auto-exposure algorithm of the spectrograph achieves high signal to noise at low tangent altitude with short exposure times such that the spacing of the measured spectra is
20 closer in tangent altitude near the bottom of the scan. Typically the spacing ranges from 1.0 km at low tangent altitude to 2.5 km at upper tangent altitudes. In the SaskMART algorithm the altitudes at which the update factor α_j is calculated correspond directly to the tangent altitudes of the lines of sight, j , in the OSIRIS scan.

Therefore, after each iteration of the SaskMART equation the ozone profile in the
25 SASKTRAN model is updated by interpolating α_j as function of altitude to the SASK-

Title Page

Abstract

Introduction

Conclusions

References

Tables

Figures

◀

▶

◀

▶

Back

Close

Full Screen / Esc

Printer-friendly Version

Interactive Discussion



TRAN shell altitudes and multiplying the ozone profile at these shell altitudes by the interpolated value of α_j . Furthermore, the multiplicative factor used for the highest retrieved altitude is applied to the profile at all altitudes above this point. Similarly, the multiplicative factor used for the lowest retrieved altitude is applied for all points below this altitude. For this work, SASKTRAN vertical shell spacing is 1 km and the altitude range extends from 0 to 100 km.

4.3 Other parameters

It has been shown in previous work that the limb scatter ozone retrieval is dependent on knowledge of the stratospheric aerosol profile and the NO_2 profile. The sulphate aerosol number density profiles used in the SASKTRAN model have been retrieved using the OSIRIS data with the technique outlined in [Bourassa et al. \(2007\)](#). The NO_2 number density was also retrieved from the OSIRIS data using a method based on the SaskMART algorithm. Details of the NO_2 retrieval will be presented in a future work.

A basic cloud detection algorithm is implemented using a long wavelength channel. The presence of a cloud top above 10 km altitude defines the lower boundary of the inversion. Also, a retrieval of the effective albedo is performed for each scan, see [Bourassa et al. \(2007\)](#). For this implementation, the initial guess ozone profile is taken from a standard climatology ([McPeters et al., 1997](#)).

4.4 A note on the error analysis

There have been recent papers that have addressed the sensitivity analysis of limb scattering ozone retrieval (e.g. [Loughman et al., 2005](#)) and those results, e.g. the effects of albedo, aerosol, pointing, etc., are also valid for the SaskMART inversion technique and need not be repeated here. More specifically, however, a methodology for performing a formal error analysis for the SaskMART technique has been presented in [Roth et al. \(2007\)](#) and [Bourassa et al. \(2007\)](#) using a numerical perturbation technique for the calculation of the required matrices. The results for this extended retrieval tech-

Title Page

Abstract

Introduction

Conclusions

References

Tables

Figures

◀

▶

◀

▶

Back

Close

Full Screen / Esc

Printer-friendly Version

Interactive Discussion



nique are very similar to those presented in Roth et al. (2007); however, the addition of the ultraviolet wavelength information keeps the uncertainty due to the measurement noise below approximately 5% up to 55 km altitude. The effect of the initial guess and the number of iterations are nearly identical to the results presented in Roth et al. (2007).

5 Results: SAGE II comparisons

In order to evaluate this inversion technique as applied to the OSIRIS data, we have selected a set of coincidences between OSIRIS limb scans and Stratospheric Aerosol and Gas Experiment (SAGE) II occultation events. For a description of the SAGE II data set see, for example, Cunnold et al. (1989), Chu et al. (1989), and McCormick et al. (1989). The coincidence set spans the almost four year mission overlap, from 2001 to 2005, and includes 196 events that are within 200 km and 2 h. The locations of the measurements are relatively well distributed over both hemispheres, from 20 to 80° latitude, and are limited to solar zenith angles at the OSIRIS tangent point that are less than 88°. Coincidences in the tropics do not occur with these tight criteria.

Figure 5 shows the SAGE II and OSIRIS SaskMART ozone profiles for a sample of four of these coincidences. These results are very typical and were chosen specifically at different latitudes to demonstrate the similarity in the structure of the retrieved profiles from the two instruments. It should also be noted that the OSIRIS retrievals appear to be very consistent through the 20 to 40 km altitude region where the information in the inversion transitions from visible to ultraviolet wavelengths.

The statistics that were generated using all 196 profiles in the coincidence set are shown in Fig. 6. For this comparison, the SAGE II profiles are convolved to 2 km resolution to better match the OSIRIS vertical resolution and interpolated to the 1 km OSIRIS retrieval grid. The left panel in the figure shows the mean of the percent difference from each coincidence and, between 18 and 53 km, it is less than 2%. Variability in time and space is likely the cause of the larger bias below 18 km. The standard deviation of the

MART Limb Scatter Ozone Retrieval

D. A. Degenstein et al.

Title Page

Abstract

Introduction

Conclusions

References

Tables

Figures

◀

▶

◀

▶

Back

Close

Full Screen / Esc

Printer-friendly Version

Interactive Discussion



percent difference from each coincidence is shown in the right panel of the figure and it is approximately a consistent 5% from 20 to 50 km. Again, it is important to note that the transitions between wavelengths in the inversion as a function of altitude do not appear in the mean bias or in the standard deviation in these comparisons with SAGE II.

The retrievals at tropical latitudes were compared in a zonal average sense due to the rare time and space coincidence between the two instruments in this region. Over a 24 h period beginning on 10 October 2003, 15 SAGE II events and 26 OSIRIS scans fall in a latitude band between 16 and 21° N. The left panel of Fig. 7 shows the percent difference between the mean profile measured by each instrument. The right panel shows the standard deviation of the profiles as an indication of the measured variability. The results are similar to the previous case with a mean bias of less than 5% from 20 to 50 km. It is likely that the agreement does not extend quite as low in this case due to the higher altitude of the tropical tropopause. This can certainly also be seen in the sharp increase in the variability of the profiles below 20 km. Overall, the variability of the measured profiles is very similar between the two instrument from 20 to 50 km. However, the slight increase in the SAGE II results as altitude approaches 50 km does not appear in the OSIRIS measurements. Once more the transition between the Chappuis and Hartley-Huggins band absorption information in the OSIRIS retrievals does not appear as a systematic bias or as an increase in the variability of the measurements.

6 Conclusions

The SaskMART technique provides a method for the retrieval of vertical profiles of ozone from limb scattered sunlight spectra that allows for the consistent incorporation of information from the Chappuis and Hartley-Huggins band absorption features as a function of altitude. A set of weighting factors is used to determine the importance of each line of sight and each element of the measurement vector for the retrieved

MART Limb Scatter Ozone Retrieval

D. A. Degenstein et al.

Title Page

Abstract

Introduction

Conclusions

References

Tables

Figures

◀

▶

◀

▶

Back

Close

Full Screen / Esc

Printer-friendly Version

Interactive Discussion



state at each altitude. The application of the technique to the measurements made by the OSIRIS instrument demonstrates agreement with coincident SAGE II occultation measurements to within 2% from 18 to 53 km altitude over a large range of geolocations and solar zenith angles.

5 This retrieval is regularly processed at the University of Saskatchewan for all OSIRIS stratospheric limb scan measurements. Data from November, 2001, to the current date is available for download as an OSIRIS Level 2 Product in HDF-EOS5 format. OSIRIS remains fully operational and processing of this algorithm will be maintained into the foreseeable future.

10 *Acknowledgements.* This work was supported by the Natural Sciences and Engineering Research Council (Canada) and the Canadian Space Agency. Odin is a Swedish-led satellite project funded jointly by Sweden (SNSB), Canada (CSA), France (CNES) and Finland (Tekes).

References

- 15 Bourassa, A. E., Degenstein, D. A., Gattinger, R. L., and Llewellyn, E. J.: Stratospheric aerosol retrieval with OSIRIS limb scatter measurements, *J. Geophys. Res.*, 112, D10217, doi:10.1029/2006JD008079, 2007. [11858](#), [11864](#)
- Bourassa, A. E., Degenstein, D. A., and Llewellyn, E. J.: SASKTRAN: A spherical geometry radiative transfer code for efficient estimation of limb scattered sunlight, *J. Quant. Spectros. Ra.*, 109, 52–73, 2008. [11863](#)
- 20 Bovensmann, H., Burrows, J. P., Buchwitz, M., Frerick, J., Noël, S., Rozanov, V. V., Chance, K. V., and Goede, A. P. H.: SCIAMACHY: Mission Objectives and Measurement Modes, *J. Atmos. Sci.*, 56, 127–150, 1999. [11855](#)
- Burrows, J. P., Richter, A., Dehn, A., Deters, B., Himmelmann, S., Voigt, S., and Orphal, J.: Atmospheric remote sensing reference data from GOME-2, Temperature dependent absorption cross sections of O₃ in the 234–794 nm range, *J. Quant. Spectrosc. Ra.*, 61, 509–519, 1999. [11863](#)
- 25 Chahine, M. T.: A General Relaxation Method for Inverse Solution of the Full Radiative Transfer Equation, *J. Atmos. Sci.*, 29, 741–747, 1972. [11857](#)

Title Page

Abstract

Introduction

Conclusions

References

Tables

Figures

◀

▶

◀

▶

Back

Close

Full Screen / Esc

Printer-friendly Version

Interactive Discussion



**MART Limb Scatter
Ozone Retrieval**

D. A. Degenstein et al.

Title Page

Abstract

Introduction

Conclusions

References

Tables

Figures

◀

▶

◀

▶

Back

Close

Full Screen / Esc

Printer-friendly Version

Interactive Discussion



- Chu, W. P., McCormick, M. P., Lenoble, J., Brogniez, C., and Pruvost, P.: SAGE II inversion algorithm, *J. Geophys. Res.*, 94, 8339–8351, 1989. [11865](#)
- Cunnold, D. M., Chu, W. P., McCormick, M. P., Veiga, R. E., and Barnes, R. A.: Validation of SAGE II ozone measurements, *J. Geophys. Res.*, 94, 8447–8460, 1989. [11865](#)
- 5 Degenstein, D. A., Llewellyn, E. J., and Lloyd, N. D.: Volume emission rate tomography from a satellite platform, *Appl. Optics*, 42, 1441–1450, 2003. [11858](#)
- Degenstein, D. A., Llewellyn, E. J., and Lloyd, N. D.: Tomographic retrieval of the oxygen infrared atmospheric band with the OSIRIS infrared imager, *Can. J. Phys.*, 82, 501–515, 2004. [11858](#)
- 10 Flittner, D. E., Bhartia, P. K., and Herman, B. M.: O₃ profiles retrieved from limb scatter measurements: Theory, *Geophys. Res. Lett.*, 27, 2601–2604, doi:10.1029/1999GL011343, 2000. [11856](#), [11857](#)
- Flynn, L. E., Homstein, J., and Hilsenrath, E.: The ozone mapping and profiler suite (OMPS). The next generation of US ozone monitoring instruments, in: *Proceedings Quadrennial Ozone Symposium*, edited by: Zerefos, C., 538–539, 2004. [11855](#)
- 15 Llewellyn, E. J., Lloyd, N. D., Degenstein, D. A., Gattinger, R. L., Petelina, S. V., Bourassa, A. E., Wiensz, J. T., Ivanov, E. V., McDade, I. C., Solheim, B. H., McConnell, J. C., Haley, C. S., von Savigny, C., Sioris, C. E., McLinden, C. A., Griffioen, E., Kaminski, J., Evans, W. F., Puckrin, E., Strong, K., Wehrle, V., Hum, R. H., Kendall, D. J. W., Matsushita, J., Murtagh, D. P., Brohede, S., Stegman, J., Witt, G., Barnes, G., Payne, W. F., Piché, L., Smith, K., Warshaw, G., Deslauniers, D.-L., Marchand, P., Richardson, E. H., King, R. A., Wevers, I., McCreath, W., Kyrölä, E., Oikarinen, L., Leppelmeier, G. W., Auvinen, H., Mégie, G., Hauchecorne, A., Lefèvre, F., de La Nöe, J., Ricaud, P., Frisk, U., Sjöberg, F., von Schéele, F., and Nordh, L.: The OSIRIS instrument on the Odin spacecraft, *Can. J. Phys.*, 82, 411–422, 2004. [11856](#)
- 20 Loughman, R. P., Griffioen, E., Oikarinen, L., Postlyakov, O. V., Rozanov, A., Flittner, D. E., and Rault, D. F.: Comparison of radiative transfer models for limb-viewing scattered sunlight measurements, *J. Geophys. Res.*, 109, doi:10.1029/2003JD003854, 2004. [11863](#)
- Loughman, R. P., Flittner, D. E., Herman, B. M., Bhartia, P. K., Hilsenrath, E., and McPeters, R. D.: Description and sensitivity analysis of a limb scattering ozone retrieval algorithm, *J. Geophys. Res.*, 110, D19301, doi:10.1029/2004JD005429, 2005. [11864](#)
- 30 McCormick, M. P., Zawodny, J. M., Veiga, R. E., Larsen, J. C., and Wang, P. H.: An overview of sage I and II ozone measurements, *Plan. Sp. Sci.*, 37, 1567–1586, 1989. [11865](#)
- McPeters, R. D., Labow, G. J., and Johnson, B. J.: A satellite-derived ozone climatology for

balloonsonde estimation of total column ozone, *J. Geophys. Res.*, 102, 8875–8886, doi:10.1029/96JD02977, 1997. [11864](#)

5 McPeters, R. D., Janz, S. J., Hilsenrath, E., Brown, T. L., Flittner, D. E., and Heath, D. F.: The retrieval of O₃ profiles from limb scatter measurements: Results from the Shuttle Ozone Limb Sounding Experiment, *Geophys. Res. Lett.*, 27, 2597–2600, doi:10.1029/1999GL011342, 2000. [11854](#)

10 Murtagh, D., Frisk, U., Merino, F., Ridal, M., Jonsson, A., Stegman, J., Witt, G., Eriksson, P., Jiménez, C., Megie, G., de La Noë, J., Ricaud, P., Baron, P., Pardo, J. R., Hauchcorne, A., Llewellyn, E. J., Degenstein, D. A., Gattinger, R. L., Lloyd, N. D., Evans, W. F. J., McDade, I. C., Haley, C. S., Sioris, C., von Savigny, C., Solheim, B. H., McConnell, J. C., Strong, K., Richardson, E. H., Leppelmeier, G. W., Kyrölä, E., Auvinen, H., and Oikarinen, L.: Review: An overview of the Odin atmospheric mission, *Can. J. Phys.*, 80, 309–319, 2002. [11856](#)

Rault, D. F.: Ozone profile retrieval from Stratospheric Aerosol and Gas Experiment (SAGE III) limb scatter measurements, *J. Geophys. Res.*, 110, doi:10.1029/2004JD004970, 2005. [11855](#)

15 Roth, C., Degenstein, D., Bourassa, A., and Llewellyn, E.: The retrieval of vertical profiles of the ozone number density using Chappuis band absorption information and a multiplicative algebraic reconstruction technique, *Can. J. Phys.*, 85, 1225–1243, 2007. [11858](#), [11859](#), [11860](#), [11864](#), [11865](#)

20 Rusch, D. W., Mount, G. H., Barth, C. A., Thomas, R. J., and Callan, M. T.: Solar mesospheric explorer ultraviolet spectrometer: Measurements of ozone in the 1.0–0.1 mbar region, *J. Geophys. Res.*, 89, 11 677–11 687, 1984. [11854](#)

25 von Savigny, C., Haley, C. S., Sioris, C. E., McDade, I. C., Llewellyn, E. J., Degenstein, D., Evans, W. F. J., Gattinger, R. L., Griffioen, E., Kyrölä, E., Lloyd, N. D., McConnell, J. C., McLinden, C. A., Mégie, G., Murtagh, D. P., Solheim, B., and Strong, K.: Stratospheric ozone profiles retrieved from limb scattered sunlight radiance spectra measured by the OSIRIS instrument on the Odin satellite, *Geophys. Res. Lett.*, 30, doi:10.1029/2002GL016401, 2003. [11855](#), [11857](#)

**MART Limb Scatter
Ozone Retrieval**

D. A. Degenstein et al.

Title Page

Abstract

Introduction

Conclusions

References

Tables

Figures

◀

▶

◀

▶

Back

Close

Full Screen / Esc

Printer-friendly Version

Interactive Discussion



MART Limb Scatter Ozone Retrieval

D. A. Degenstein et al.

Table 1. Definitions of the 9 pair/triplet combinations calculated from the measured limb radiances shown in Fig. 1 that are used to construct the measurement vector, y_{jk} .

	y_{j0}	y_{j1}	y_{j2}	y_{j3}	y_{j4}	y_{j5}	y_{j6}	y_{j7}	y_{j8}
Definition	Pair	Pair	Pair	Pair	Pair	Pair	Pair	Triplet	Triplet
Absorbing Wavelength (nm)	292	302	306	309	315	322	331	599	602
Reference Wavelength 1 (nm)	351	351	351	351	351	351	351	540	544
Reference Wavelength 2 (nm)	–	–	–	–	–	–	–	668	679
Minimum Altitude (km)	47	42	40	37	31	24	18	–	–
Maximum Altitude (km)	60	60	54	50	44	40	37	28	28
Normalization Altitude (km)	65	65	59	55	49	45	42	33	33

[Title Page](#)
[Abstract](#)
[Introduction](#)
[Conclusions](#)
[References](#)
[Tables](#)
[Figures](#)
[I◀](#)
[▶I](#)
[◀](#)
[▶](#)
[Back](#)
[Close](#)
[Full Screen / Esc](#)
[Printer-friendly Version](#)
[Interactive Discussion](#)


MART Limb Scatter
Ozone Retrieval

D. A. Degenstein et al.

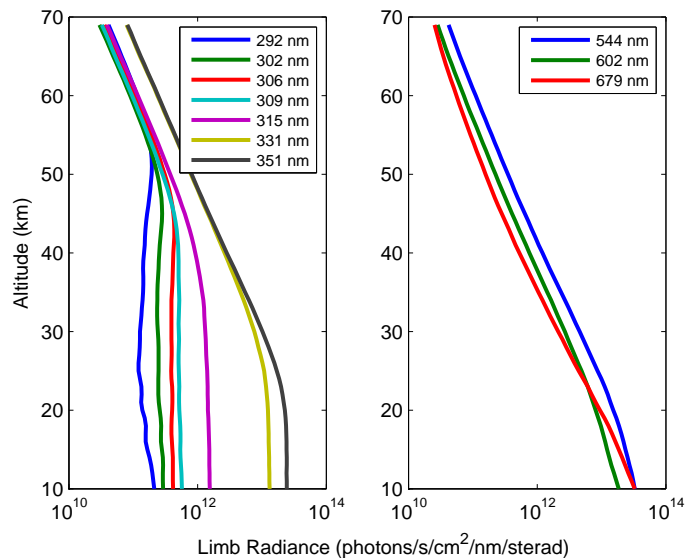


Fig. 1. A sample set of OSIRIS limb radiance profiles used for the ozone retrieval. Measurements within the Hartley-Huggins band and Chappuis band are shown in the left and right panels, respectively.

[Title Page](#)[Abstract](#)[Introduction](#)[Conclusions](#)[References](#)[Tables](#)[Figures](#)[◀](#)[▶](#)[◀](#)[▶](#)[Back](#)[Close](#)[Full Screen / Esc](#)[Printer-friendly Version](#)[Interactive Discussion](#)

**MART Limb Scatter
Ozone Retrieval**

D. A. Degenstein et al.

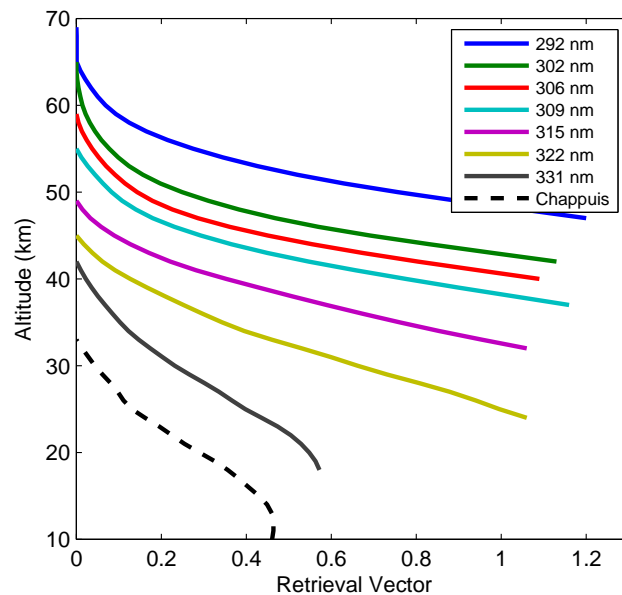


Fig. 2. A sample set of the 9 OSIRIS pair/triplet measurement vector elements used in the ozone retrieval. See Table 1 for complete definitions. Values of the two Chappuis triplets are indistinguishable in this plot.

[Title Page](#)[Abstract](#)[Introduction](#)[Conclusions](#)[References](#)[Tables](#)[Figures](#)[◀](#)[▶](#)[◀](#)[▶](#)[Back](#)[Close](#)[Full Screen / Esc](#)[Printer-friendly Version](#)[Interactive Discussion](#)

**MART Limb Scatter
Ozone Retrieval**

D. A. Degenstein et al.

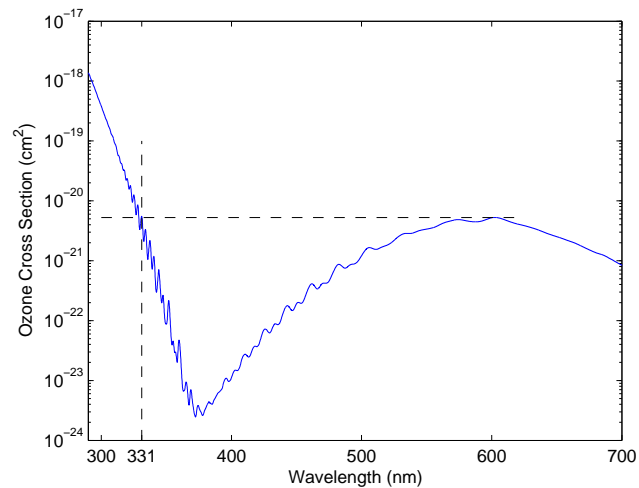


Fig. 3. Typical ozone absorption cross section. The value is similar at 331 nm and 602 nm.

[Title Page](#)[Abstract](#)[Introduction](#)[Conclusions](#)[References](#)[Tables](#)[Figures](#)[◀](#)[▶](#)[◀](#)[▶](#)[Back](#)[Close](#)[Full Screen / Esc](#)[Printer-friendly Version](#)[Interactive Discussion](#)

**MART Limb Scatter
Ozone Retrieval**

D. A. Degenstein et al.

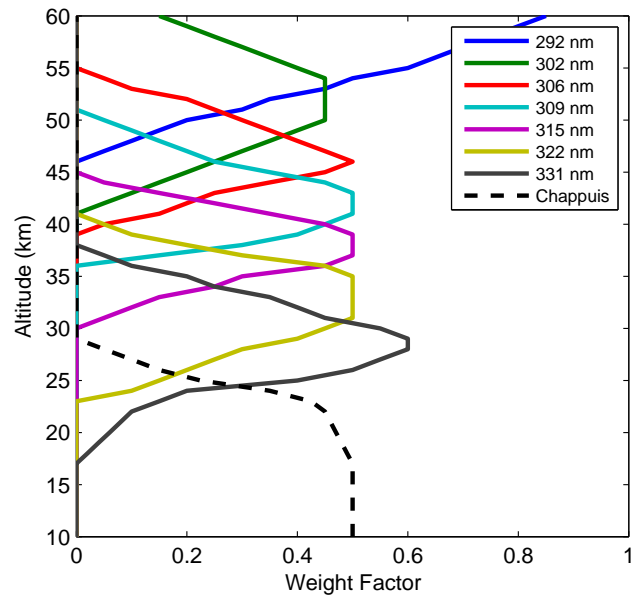


Fig. 4. The weighting factors assigned to each of the vectors as a function of altitude.

[Title Page](#)[Abstract](#)[Introduction](#)[Conclusions](#)[References](#)[Tables](#)[Figures](#)[◀](#)[▶](#)[◀](#)[▶](#)[Back](#)[Close](#)[Full Screen / Esc](#)[Printer-friendly Version](#)[Interactive Discussion](#)

MART Limb Scatter
Ozone Retrieval

D. A. Degenstein et al.

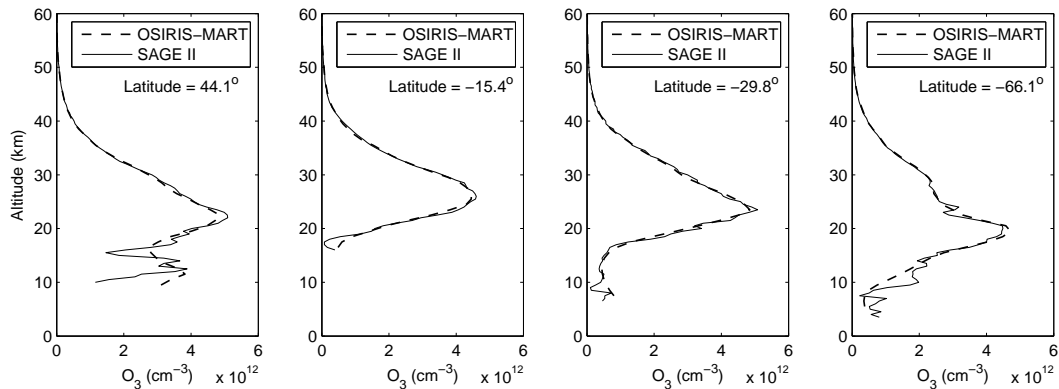


Fig. 5. A selection of single profiles that meet the coincidence criteria. Profiles are shown at their inherent vertical resolution. The entire data set consists of 196 coincidences.

[Title Page](#)[Abstract](#)[Introduction](#)[Conclusions](#)[References](#)[Tables](#)[Figures](#)[◀](#)[▶](#)[◀](#)[▶](#)[Back](#)[Close](#)[Full Screen / Esc](#)[Printer-friendly Version](#)[Interactive Discussion](#)

**MART Limb Scatter
Ozone Retrieval**

D. A. Degenstein et al.

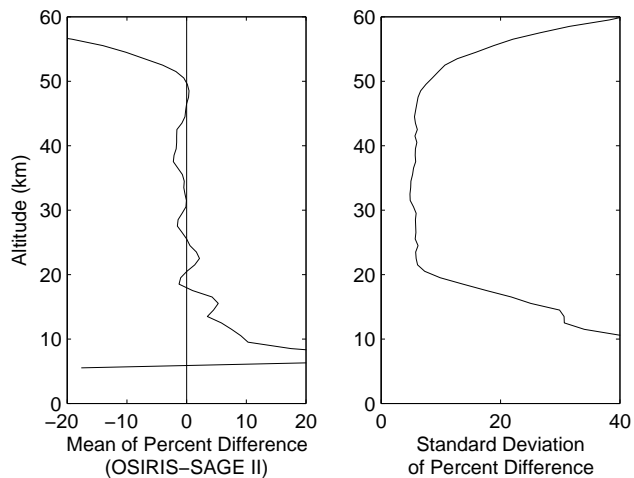


Fig. 6. The mean and standard deviation of the percent differences between the retrieved ozone profiles for 196 coincident OSIRIS and SAGE II measurements.

[Title Page](#)[Abstract](#)[Introduction](#)[Conclusions](#)[References](#)[Tables](#)[Figures](#)[I◀](#)[▶I](#)[◀](#)[▶](#)[Back](#)[Close](#)[Full Screen / Esc](#)[Printer-friendly Version](#)[Interactive Discussion](#)

MART Limb Scatter
Ozone Retrieval

D. A. Degenstein et al.

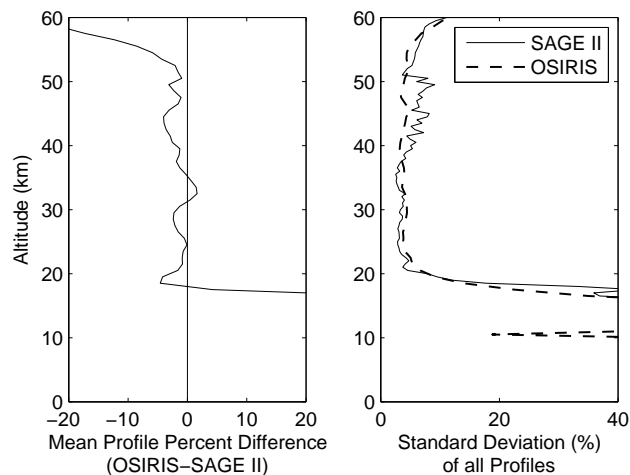


Fig. 7. The percent difference of the zonal average profile measured by OSIRIS and SAGE II over 24 h for a 5° tropical latitude band (15 SAGE II measurements and 26 OSIRIS measurements).

[Title Page](#)[Abstract](#)[Introduction](#)[Conclusions](#)[References](#)[Tables](#)[Figures](#)[I◀](#)[▶I](#)[◀](#)[▶](#)[Back](#)[Close](#)[Full Screen / Esc](#)[Printer-friendly Version](#)[Interactive Discussion](#)